

Amine-Rich Cell-Culture Surfaces for Research in Orthopedic Medicine

Fackson Mwale,^{1,*} Sonia Rampersad,¹ Juan-Carlos Ruiz,² Pierre-Luc Girard-Lauriault,² Alain Petit,¹ John Antoniou,¹ Sophie Lerouge,³ & Michael R. Wertheimer²

¹Division of Orthopaedic Surgery, McGill University, and Lady Davis Institute for Medical Research;

²Department of Engineering Physics, École Polytechnique, Montreal; ³Department of Mechanical Engineering, École de Technologie Supérieure (ÉTS)

*Address all correspondence to: Fackson Mwale, Division of Orthopaedic Surgery, McGill University, and Lady Davis Institute for Medical Research, 3755, Chemin de la Cote Ste-Catherine, Montreal, QC H3T 1E2, Canada; Tel: 514-340-8222 ext 2948; Fax: 514-340-7502; fmwale@ldi.jgh.mcgill.ca

ABSTRACT: We report results of ongoing research relating to cell immobilization and cell culture on bioactive organic coatings deposited using three different techniques—two plasma assisted, the third based on vacuum-ultraviolet photo-polymerization. We start by briefly comparing those three methods and by describing some of the key characteristics of the resulting coatings; all are designed to be rich in primary amines, a functional group known to be highly bioactive. Next, we focus on two cell types of importance to long-term objectives in our orthopedic research laboratory: (i) The first, nonadherent human U937 monocytes, is a cell line that has been widely used as a model of the mammalian cellular response to various inflammatory stimuli, and in understanding the clinical relevance of elevated cobalt and chromium levels in patients with metal-on-metal total hip arthroplasty and hip resurfacing arthroplasty. (ii) The second cell type, adherent human mesenchymal stem cells (MSCs), derived from patients suffering from osteoarthritis (OA), is important in biological repair of cartilage and of the degenerate intervertebral disc (IVD) from the patients' autologous cells. Much progress has been achieved in both cases, as illustrated with results based to a considerable extent on real-time reverse-transcription (RT) polymerase chain reaction (PCR), a key methodology used in this type of research.

KEY WORDS: Primary amine, Cell-culture, Orthopedic medicine

I. INTRODUCTION

In recent years, plasma technologies have been extensively used to alter the surface properties of synthetic polymers, so as to elicit desired responses toward biological environments.^{1–3} Those studies comprised either surface functionalization (so-called grafting),^{1–6} or plasma polymerization (PP), which involves adding a thin organic coating on top of the original surface.^{1–3,6–11} Physicochemical properties of both types of newly created surfaces—chemical functionality, surface energy, roughness, surface charge, etc.—are believed to govern their interactions with a given biological environment. In this paper, we shall focus exclusively on thin film coatings. An important class of functional coatings are nitrogen (N)-rich ones,^{1,2,6–16} which have been found to promote cell adhesion,^{6,7,12–16} and even to influence differentiation of human mesenchymal stem cells (MSCs),^{14,15} topics to be addressed in the present article. This is presumed to be due to

the presence of primary amine groups, C-NH_2 , and their associated positive charges that may, in aqueous solutions at physiological pH values, attract negatively charged biomolecules (proteins, DNA) and thus, directly or indirectly, living cells.^{1-3,6,12-16} Moreover, such amino groups are chemically reactive, and they are used in biochemistry for covalent coupling of proteins in aqueous environments.^{1-3,6} In the category of graft-modified polymer surfaces, commercial polystyrene culture dishes are generally pretreated in atmospheric air plasma, and they therefore comprise oxygen (O)-based functionalities with typical concentrations, [O], in the vicinity of 18 atomic % (at. %).

If one elects to work with an aminated organic coating (e.g., a plasma polymer), the deposit must have a sufficiently high density of primary/secondary amines to become positively charged in aqueous media, and to enable imine and enamine coupling.¹¹ In addition, such a surface layer must be stable in the aqueous media routinely used for cell culture. These two requirements are frequently in conflict, and numerous earlier attempts to increase the density of amine groups, $[-\text{NH}_2]$, by lowering average plasma power led to water-soluble films.^{1,6,17} Well-known routes for obtaining coatings with high surface concentrations of nitrogen, [N], are plasma polymerization of suitable N-containing precursors (e.g., allylamine, AA),^{1,2,6,9-11,17-21} or the mixture of hydrocarbon and N-containing gases.^{7,8,22-27} In a recently published article,²⁸ we focused on fabrication of PE:N (N-containing polyethylene) films from binary feed-gas mixtures comprising ethylene (C_2H_4) and N_2 or ammonia (NH_3), leading to the most stable deposits. More precisely, we examined two kinds of PPE:N (N-rich plasma-polymerized ethylene), namely those obtained either by conventional low-pressure (L) radio-frequency (r.f.) glow discharge, hereafter designated L-PPE:N,^{25,29} or in a dielectric barrier discharge (DBD) reactor operating at atmospheric (H, for high) pressure (hereafter H-PPE:N).^{7,8,29} A third category of coatings, designated UV-PE:N, results from vacuum-ultraviolet (VUV) photo-polymerization reactions in the same gas mixtures as those used for producing the L-PPE:N films. UV-PE:N films are also prepared at low pressures, but in a reactor dedicated for VUV-photochemical research, mostly using a commercial Kr lamp emitting monochromatic radiation at 123.6 nm.²⁶ L-PPE:N and UV-PE:N films are *a priori* more costly to produce on account of the more expensive vacuum processing and equipment and, in the photochemical case, the expensive light source. However, in high value-added processes, for example those involving biomaterials and substrates for tissue engineering, production costs are not necessarily the dominating consideration, usually less so than performance characteristics of the types that are the focus of investigations described in this paper.

As already briefly mentioned above, we shall address two important applications of PE:N coatings in the remainder of this text:

- (i) Adhesion of U937 monocytes,^{7,13}
- (ii) Regeneration of cartilage via the use of mesenchymal stem cells (MSC) from osteoarthritic (OA) patients.^{14,15}

Both of these topics are of very great interest within our orthopedics research program, but for quite different reasons and within different contexts: In the former case,

the blood-borne human U937 cells, precursors for the formation of macrophages, were nonadhering to all then-known culture surfaces prior to investigations in these laboratories. This had been a distinct obstacle when pursuing research into the mechanisms of periprosthetic osteolysis, a loosening of artificial hip implants due to apoptosis or necrosis of osteoblasts.^{30,31} Thanks to their adherence to PE:N under certain conditions described later in this text, that obstacle has now been largely overcome.

Regarding the second topic listed above, several studies have been directed toward using MSCs from OA patients for the repair of cartilage and of the degenerate intervertebral disc (IVD), not only because these are the patients that will require a source of autologous stem cells if biological repair of cartilage or IVD lesions is to be a therapeutic option, but also to help further understanding of stem cell differentiation. However, recent evidence indicates that a major drawback of current cartilage or IVD tissue engineering is that human MSCs from these patients express type X collagen (COL X),^{14,15,32} a marker of chondrocyte hypertrophy associated with endochondral ossification.^{33,34}

We have earlier published (or submitted) many of our important findings regarding both (i) and (ii) above; however, in the present article we present hitherto unreported views regarding the likely mechanisms underlying the adhesion and colonization of these two cell types of importance in orthopedic medicine, when they are cultured on PE:N surfaces.

II. EXPERIMENTAL METHODOLOGY

A. Deposition of PE:N Films

PE:N films were deposited in the three reactor systems depicted in Fig. 1, on two types of polymer substrates, namely biaxially oriented poly(propylene) (BOPP, 50 μm thick, isotactic polymer film, graciously provided by 3M Company, St. Paul, MN), and 50 μm thick PET film obtained from Goodfellow Corp. (Oakdale PA). Surface analyses (see below) were conducted to verify that the deposition rates and chemical compositions of PE:N deposits were independent of their host surfaces.

The L-PPE:N coatings were deposited in a cylindrical aluminum/steel vacuum chamber, approximately 20 cm in diameter and 20 cm in height, Fig. 1a.^{25,29} Flows of high-purity feed gases (ethylene 99.5% and ammonia 99.99%, Air Liquide Canada, Montreal, QC) were admitted into the chamber using electronic flow meter/controllers (Vacuum General Inc., San Diego, CA), and a “shower head” gas distributor (10 cm in diameter). While the flow rate of C_2H_4 “monomer,” $F_{\text{C}_2\text{H}_4}$, was kept constant at 20 standard cubic centimeters per minute (sccm), its NH_3 counterpart, F_{NH_3} , could be varied between 0 and 60 sccm.²⁵ Based on our previous experience, we chose to deposit L-PPE:N coatings using rather mild plasma conditions ($P = 10$ W, resulting in a negative d.c. bias voltage, $V_B = -40$ V); under these conditions, polymer-like films with maximum nitrogen and amine concentrations were deposited.^{25,29} Based on previous work relating to stability of the deposits in air and water,²⁸ we chose in the present studies to prepare particular coatings with $F_{\text{NH}_3} = 15$ and 20 sccm, that is, with ratios $R = F_{\text{NH}_3}/F_{\text{C}_2\text{H}_4}$ of 0.75 and 1, respectively

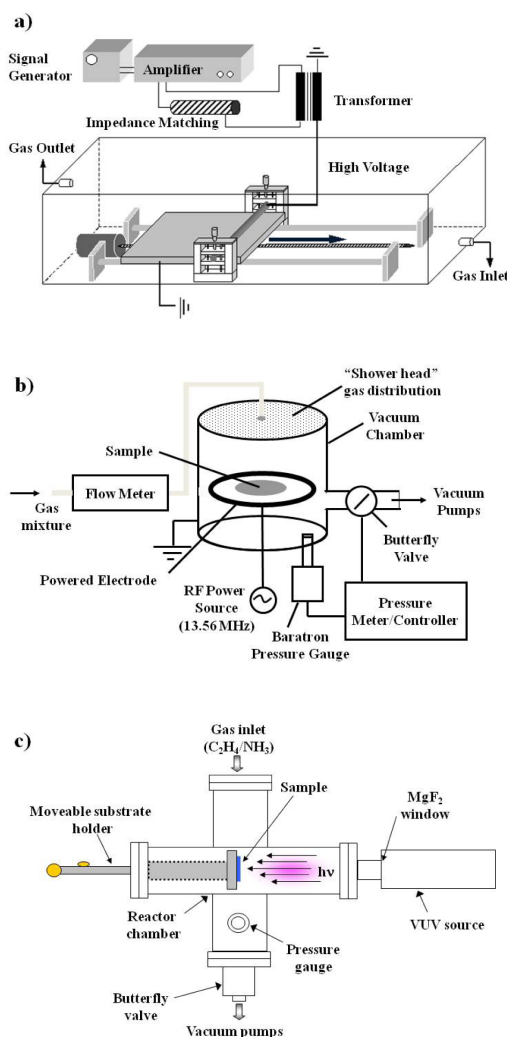


FIGURE 1. Three reactor systems used in the present research: (a) Low-pressure plasma (LP-PECVD), 13.56 MHz r.f. discharge; (b) Atmospheric-pressure dielectric barrier discharge (AP-DBD) plasma; (c) Vacuum ultraviolet photo-polymerization (VUV-CVD), see text. (From ref. 28, with permission.)

(hereafter identified as L0.75 and L1). Indeed, unless otherwise specified, all of the data relating to experiments with MSCs were carried out with the L0.75 coating.

For the case of H-PPE:N, deposition was carried out in a DBD reactor, as also described elsewhere.^{7,8,28,29} Briefly, this system (Fig. 1b) comprised a cylindrical, dielectric-coated stainless steel high-voltage (HV) electrode and a horizontal, grounded planar aluminum (Al) electrode, covered by a 2-mm-thick glass plate that served as a second dielectric layer. The precursor gas mixture, $X = F_{N_2}/F_{C_2H_4}$, composed of pure nitrogen (N₂) and ethylene (C₂H₄), was introduced into the discharge zone, an adjustable gap

(usually 1 mm) between the HV electrode and the glass plate. The N_2 flow rate was fixed at 10 standard liters per minute (slm); as mentioned above, deposits were made using C_2H_4 flow rates of 20 or 50 sccm for reasons of their good to superior physicochemical stability (hereafter identified as H20 and H50).²⁸ Again, unless otherwise specified, MSC-related experiments were carried out with the H50 coating.

The third experimental set-up, used for VUV photochemical experiments (see Fig. 1c) has also already been described in detail elsewhere²⁶. Briefly, it consists of a stainless steel “cross” chamber, which was first evacuated to a base pressure of about 5×10^{-6} torr ($\sim 7 \times 10^{-4}$ Pa) using a combination of turbomolecular and rotary vacuum pumps. In the present VUV photo-polymerization experiments with 123.6 nm monochromatic radiation, we irradiated flows of binary gas mixtures comprising C_2H_4 and NH_3 at low pressure, typically 100 mTorr (13.3 Pa), similar to those used for depositing L-PPE:N, described above. The flow rate of ethylene, $F_{C_2H_4}$, was kept constant at 50 sccm, while that of ammonia, F_{NH_3} , could be varied between 0 and 75 sccm, yielding values of their ratio, R ($\equiv F_{NH_3}/F_{C_2H_4}$), between 0 and 1.5. Also based on previous work relating to stability of the deposits in air and water,²⁸ we chose in the present study to prepare particular coatings with values of R ranging from $R = F_{NH_3}/F_{C_2H_4}$ of 0.4 to 1, respectively.

For all coating processes, deposition durations were selected so as to create approximately 100-nm-thick films. Elemental compositions of PE:N samples and their primary amine concentrations were determined by X-ray photoelectron spectroscopy (XPS) in a VG ESCALAB 3MkII instrument, using nonmonochromatic Mg $K\alpha$ radiation, as described in detail elsewhere.^{7,8,25,26,28,35} The near-surface concentrations of primary amines, $[-NH_2]$, were determined after chemical derivatization with 4-(trifluoromethyl) benzaldehyde (TFBA, Alfa Aesar, Ward Hill, MA) vapor. With this method, $[-NH_2]$ values can be deduced accurately from the measured fluorine concentrations, $[F]$, also by XPS.^{25,28,29} As reported previously, values of $[N]$ and $[-NH_2]$ increase significantly with increasing NH_3/C_2H_4 or N_2/C_2H_4 ratios.

In certain experiments involving the U937 cells, micropatterned arrays of PE:N islands were deposited on BOPP surfaces that were partially masked with 50- μ m-thick KaptonTM polyimide films. These masks comprised square arrays (200 μ m pitch) of small (ca. 50 μ m diameter) holes that had been eroded through the Kapton with the help of a powerful KrF excimer laser.⁷

B. Field-Emission Scanning Electron Microscopy (FE-SEM)

Selected coatings were examined by field-emission scanning electron microscopy (FE-SEM) using a JEOL model JSM-7600 TFE instrument (JEOL Ltd., Tokyo, Japan). For this purpose, relatively thick (≥ 0.5 μ m) H-PPE:N and L-PPE:N films were deposited on glass and on silicon wafers, respectively, in order to allow small (~ 1 cm²) representative pieces to be fractured in ambient air, then introduced into the microscope's sample holder. The purpose was to examine both top and side views of their micromorphologies,²⁸ but only top views are presented and discussed here.

C. Cell Culture and Real-Time RT-PCR

1. U937 Monocytes

Nonadherent human U937 monocytes (ATCC, Rockville, MD) were expanded in suspension in Dulbecco's modified Eagle's medium (DMEM; Wisent, St-Bruno, QC) high glucose supplemented with 10% fetal bovine serum (FBS; Wisent, St-Bruno, QC), 100 U/mL penicillin, and 100 µg/mL streptomycin. Cells were counted with a hemacytometer; 100-µL volumes of cell suspension (5×10^5 cells) were carefully pipetted onto 1-cm² PE:N surfaces of varying [N] values, which had previously been placed face up on the flat bottoms of wells in a 24-well cell-culture plate. Cells were then left in contact with the substrate surfaces in humidified air enriched with 5% CO₂ at 37°C for 1h before careful removal of the medium. We had previously demonstrated that the maximal adhesion of U937 cells to PE:N surfaces was reached within 1h.^{7,13} Nonadherent cells were then removed rapidly to avoid their interaction with adherent ones that might modify cell-surface interactions and gene expression. Following this, fresh medium was pipetted into the wells (1 mL in each well) and again carefully removed to wash the cells. This washing procedure was repeated twice. All of the adhesion experiments were performed at the same time with the same cell suspension, to avoid variations due to the cells.

Real-time reverse-transcription polymerase chain reaction (RT-PCR) experiments were carried out for the case of adhering cells as follows: Cells were incubated for durations ranging from 3 to 24 h on PE:N-coated BOPP, following which the total RNA was extracted with TRIzol reagent (Invitrogen, Burlington, ON). All of the RT-PCR experiments were performed at the same time with the same cell suspension, to avoid variations due to the cells. After centrifugation for 15 min at $12,000 \times g$ at 4°C, the aqueous phase was precipitated in 1 volume of isopropanol, incubated for 45 min at room temperature, and centrifuged again for 15 min at $12,000 \times g$ at 4°C. The resulting RNA pellet was washed with 75% ethanol, centrifuged, and air-dried. The pellets were suspended in 50 µL of diethylpyrocarbonate (DEPC)-treated water and assayed for RNA concentration and purity by measuring A_{260}/A_{280} . The reverse transcription (RT) reaction was performed using 1 µg total RNA after DNase I digestion according to the Invitrogen protocol. In a total volume of 20 µL, the reaction solution contained 50 mM Tris-HCl (pH 8.3), 75 mM KCl, 3 mM MgCl₂, 10 mM DTT, 50 µM each of dATP, dGTP, dCTP, and dTTP, and 200 units of Superscript II RNase H⁻ reverse transcriptase (Invitrogen). The expressions of tumor necrosis factor-α (TNF-α), interleukin-1-β (IL-1β), peroxisome proliferators-activated receptor-γ (PPARγ), intercellular adhesion molecule-1 (ICAM-1), and transcription factors Egr-1 and PU.1 were measured using a Roche Diagnostics (Laval, QC) LightCycler™, as described elsewhere.¹³ Glyceraldehyde-3-phosphate dehydrogenase (GAPDH) was used as a housekeeping gene. U937 cells in suspension served as a control. Salt-free primers for the target genes (TNF-α, IL-1β, PPARγ, ICAM-1, Egr-1, PU.1) and for the GAPDH housekeeping gene were generated by Invitrogen; their sequences are presented elsewhere, along with other procedural details.¹³ In the present article, we shall report data pertaining only to TNF-α, IL-1β.

2. Human MSCs

Human MSCs were obtained from 10- to 25-mL bone marrow aspirates from the femoral intramedullary canal of donors undergoing total hip replacement using a protocol approved by the Research Ethics Committee of the Jewish General Hospital.^{14,15,32} The marrow donors included both males and females ranging in age from 52 to 88 y (mean, 65 y). Isolation of MSCs was carried out using methods previously described.^{14,15,36} Briefly, each aspirate was diluted 1:1 with DMEM and gently layered 1:1 over Ficoll (1.073 g/ml Ficoll-Plaque; GE Healthcare, Baie d'Urfé, QC) and centrifuged at $900 \times g$ for 30 min. After centrifugation, the low-density MSC-enriched fraction was collected from the interface, supplemented to 40 mL with DMEM, and centrifuged at $600 \times g$ for 10 min. After two washes, the cells were re-suspended in 20 mL of DMEM supplemented with 10% fetal bovine serum (FBS; Wisent), 100 U/mL penicillin, 100 μ g/mL streptomycin and cultured under pre-confluency in 150-mm culture dishes at 37°C with 5% humidified CO₂. After 72 h, the nonadherent cells were discarded when changing the medium.

One million passage 3 or 4 MSCs were cultured for up to 7 d on either H-PPE:N or L-PPE:N coatings in DMEM supplemented with 10% FBS, 100 U/mL penicillin, and 100 μ g/mL streptomycin. Commercial polystyrene (PS) tissue-culture dishes (Sarstedt, Montreal, QC) were used as controls. The medium was changed every 2 d.

At the end of incubations, cells were washed with phosphate-buffered saline (PBS) and total RNA was isolated by a modification of the method of Chomczynski and Sacchi³⁷ using TRIzol reagent. After centrifugation for 15 min at $12,000 \times g$ at 4°C, RNA in the aqueous phase was precipitated with isopropanol and recovered by centrifugation for 15 min at 4°C. The resulting RNA pellet was air dried, resuspended in 40 μ L diethylpyrocarbonate-treated water, and the purity of the RNA was assessed by measuring the A_{260}/A_{280} ratio. The RT reaction was performed using 1 μ g total RNA and 200 units Superscript II RNase H- reverse transcriptase as previously described.^{14,15,32} PCR was performed in a total volume of 25 μ L with 2.5U Taq polymerase (Invitrogen), also as previously described.^{14,15,32} Primers used in the study and other procedural details are described elsewhere.^{14,15} Amplified products were analyzed by electrophoresis on 1% agarose gels and visualized by ethidium bromide staining. Quantification was carried out using Quantity One software on a VersaDoc image analysis system (Bio-Rad Laboratories, Mississauga, ON) equipped with a cooled CCD 12-bit camera.

III. RESULTS

A. Characteristics of PS Control and of PPE:N Surfaces

As already mentioned, the surfaces of commercial polystyrene (PS) tissue-culture dishes are modified by plasma treatment at the manufacturer, and they typically comprise about 18 atomic % (at. %) of bound oxygen, so as to enhance wettability and cell adhesion.

Chemical characterizations of the three families of PE:N films have been the subjects of previous articles, some dedicated to a specific family,^{7,8,25,26,29} another to all

three.²⁸ Figure 2 shows the compositions of two types of PE:N deposits used in this work, namely L-PPE:N and H-PPE:N. The total concentrations of nitrogen, [N] (in at. %), increased as a function of the gas mixture ratios, X and R , for both H- and L-PPE:N (Fig. 2a). Primary amine $[-NH_2]$ content also increased as a function of the gas mixture ratio for L-PPE:N, but remained roughly constant for H-PPE:N (Fig. 2b). The reader is reminded that for reasons of their superior chemical stability (low solubility in aqueous cell-culture media),²⁸ the following compositions were used here preferentially, unless otherwise specified:

- (i) L-PPE:N: $R = 0.75$ (L0.75);
- (ii) H-PPE:N: $X = 200$ (H50).

Although [N] values ranged from about 16 to about 24 at. % among the different materials illustrated in Fig. 2, their primary amine concentrations, $[NH_2]$, varied from 5.1

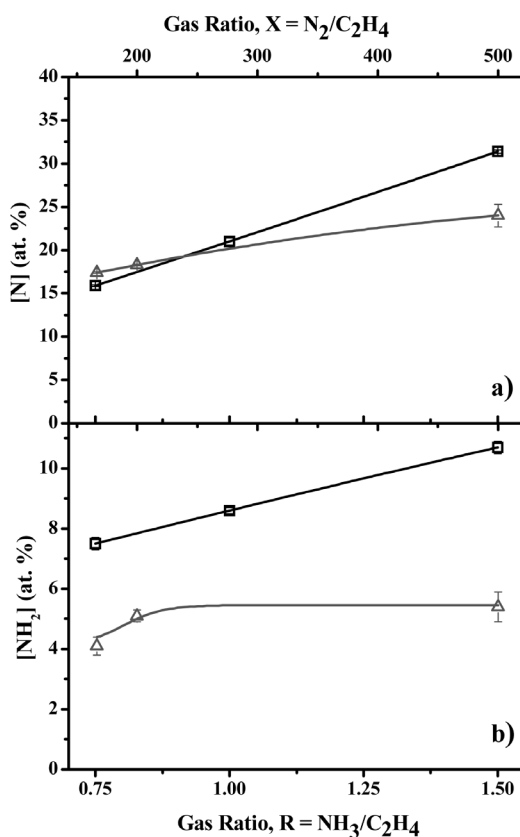


FIGURE 2. (a) Concentrations (in atomic %) of nitrogen, [N], and (b) of primary amines, $[NH_2]$, in L-PPE:N (\square) and H-PPE:N (Δ) deposits, as functions of the gas mixture ratios, $R \equiv F_{NH_3}/F_{C_2H_4}$ (for L-PPE:N), or $X \equiv F_{N_2}/F_{C_2H_4}$ (for H-PPE:N, see text). (From ref. 15, with permission.)

to 8.6 at. %, being near constant for the case of H-PPE:N, but significantly higher for the two L-PPE:N coatings. Figure 3 shows that L- and H-PPE:N coatings differed not only in their compositions, but also in their surface morphologies. Indeed, scanning electron microscopy images show that H-PPE:N coatings (Figs. 3A and 3B) possess rough surface morphologies, while their L-PPE:N counterparts, in sharp contrast, are extremely smooth (Fig. 3C). The latter also applies to UV-PE:N coatings, not illustrated here.²⁸

B. U937 Monocytes

1. “Critical” Surface Conditions for Cell Adhesion

In earlier articles,^{7,13} we have demonstrated and reported the existence of a “critical” nitrogen concentration, $[N]_{\text{crit}}$, a quite sharply defined $[N]$ value at PE:N film surfaces, below which U937 monocytes were found not to adhere at all. This is illustrated in Fig. 4A

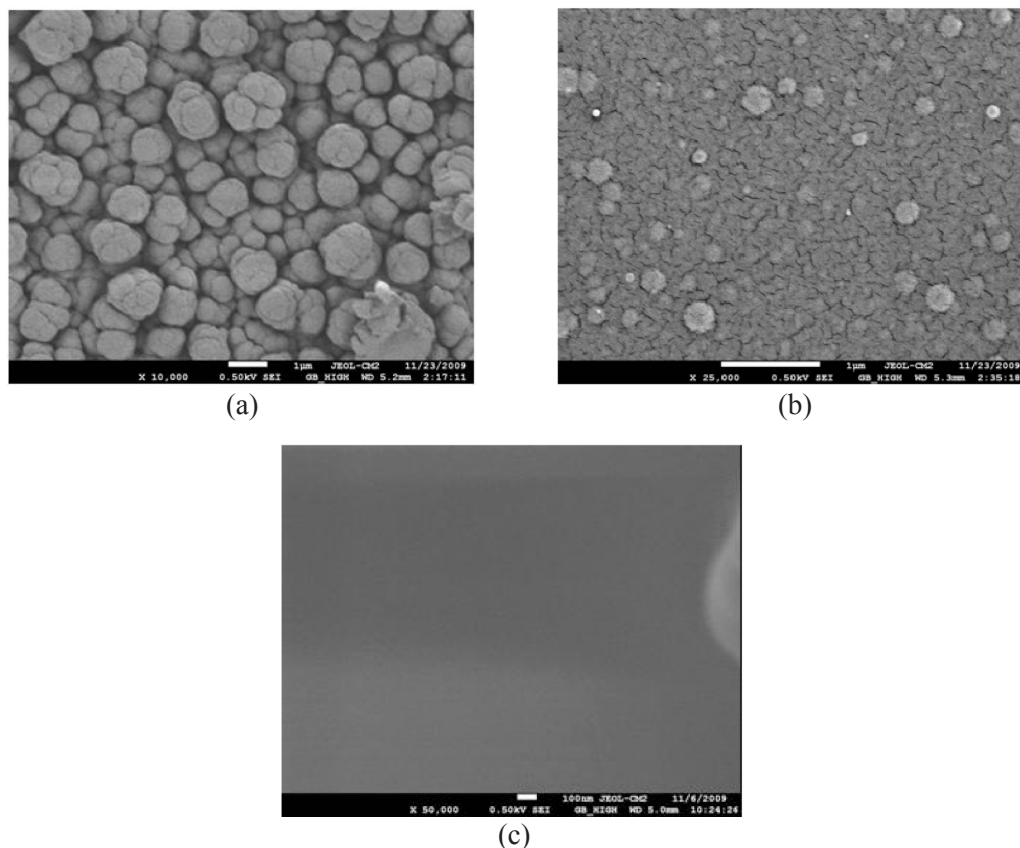


FIGURE 3. Surface morphologies of PPE:N coatings. Images of H20-PPE:N (A), H50-PPE:N (B), and L0.75-PPE:N (C) surfaces were acquired by field-emission scanning electron microscopy (FE-SEM). (After ref. 28, modified, with permission.)

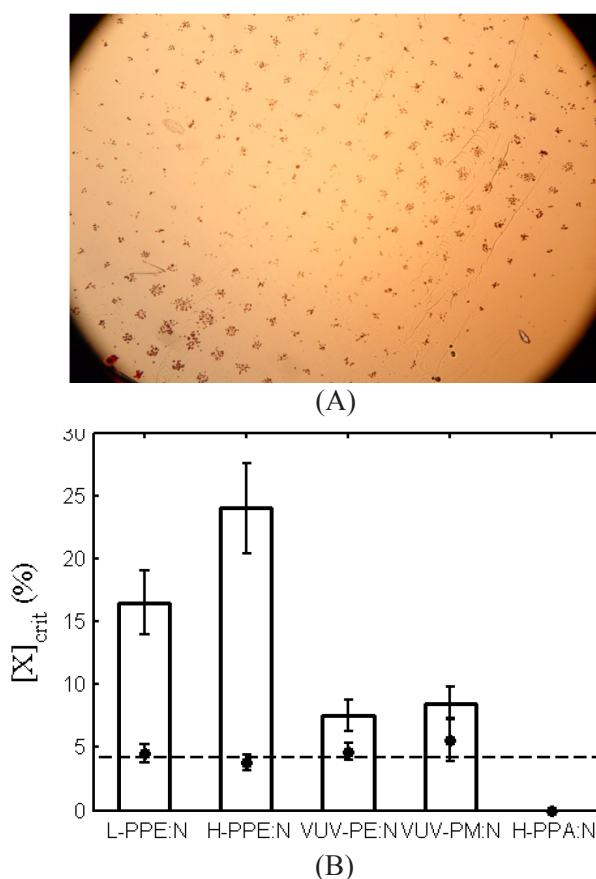


FIGURE 4. (A) Adherence of U937 cells on a micro-patterned BOPP surface comprising 50- μ m islands of H-PPE:N in a square array with 200- μ m pitch. (After ref. 7, with permission.) (B) Quantification of $[N]_{crit}$ in the adhesion experiments involving U937 cells. The “critical” nitrogen content, $[N]_{crit}$, required to stimulate adhesion of U937 monocytes to various coatings, namely: L-PPE:N, H-PPE:N, VUV-PE:N, VUV-PM:N and H-PPA:N, are shown in histogram-form. For each one of the materials, the corresponding critical amino-group content, $[NH_2]_{crit}$ (\bullet), is superimposed. The average value of $[NH_2]_{crit}$ is presented as a dashed, horizontal line. In the case of H-PPA:N, no adhesion of U937 was observed under any circumstances, in spite of high $[N]$ values. Note that the symbol $[X]$ on the ordinate axis refers to both $[N]$ and $[NH_2]$, on the same scale. (After ref. 13, with permission.)

for the case of H-PPE:N, where cells are seen to adhere only on the small PE:N islands deposited through openings in the Kapton mask, but not on the adjacent bare BOPP. Indeed, for the case of H-PPE:N, $[N]_{crit}$ was found to be 24% (ref. 13); for all values of $[N] > [N]_{crit}$, U937 cells adhered to the coatings, but not when $[N]$ values were lower.

Having stated this, let us now turn to Fig. 4B: The first three of five different coatings families examined represent PE:N, while the fourth and fifth represent deposits based on the use of methane (M) and acetylene (A) “monomers,” respectively.^{8,13} All these were seen to also exhibit sharply defined values of $[N]_{crit}$, just like H-PPE:N (with the exception of H-PPA:N, discussed below). However, the exact “critical” values varied among the different materials, ranging from 24% for H-PPE:N to 7.5% for VUV-PE:N. Thanks to the chemical derivatization experiments described earlier and illustrated in Fig. 2b, we could determine the corresponding values of $[NH_2]_{crit}$, and these are also shown plotted in Fig. 4B. Very strikingly, we note that these values of the “critical” primary amine concentrations are the same for all materials, $[NH_2]_{crit} = 4.2 \pm 0.5\%$, within the limits of experimental precision. It might be added that we have verified our procedures for measuring $[NH_2]$ with the help of a commercially available coating material that possesses a precisely known primary amine concentration, and in which all of the bound nitrogen occurs in the form of this functionality, i.e., $[NH_2]/[N] = 100\%$. This material is Parylene diX AM (aminomethyl-[2-2]paracyclophane, Kisco Conformal Coating LLC, Milford, CT), and we found the value $[NH_2]/[C]$, $6.5 \pm 0.6\%$, that almost exactly corresponds to the calculated one, 6.3 %, based on this material’s chemical structure. (Parylene diX AM coatings were graciously provided by Drs. B. Elkin and C. Oehr, Fraunhofer Institute for Interfacial Engineering and Biotechnology, Stuttgart Germany; a joint publication is currently in preparation.)

The key inference to emerge from Fig. 4B is that primary amine groups play a dominant role in the mechanism of U937 adhesion to N-rich organic surfaces. This statement receives further convincing support from the observation, also illustrated in Fig. 4B, that H-PPA:N (which can have $[N]$ up to ~40%) has $[NH_2]$ values that never exceed 2%,^{8,13} in other words, these are always below $[NH_2]_{crit}$. Therefore, this material is inherently incapable of inducing the adhesion of U937 monocytes. These results strongly support the view that $[NH_2]$, rather than simply $[N]$, which is general and does not take into account the distribution of functional groups, should be considered in film design for such bio-applications. Further circumstances that strongly support the above-stated inference are the facts that the films’ other characteristics, for example, differing $[O]$ and $[H]$ values, but primarily their very different surface morphologies (mean surface roughness, see Fig. 3), appeared to play no major roles. Possible underlying cell-adhesion mechanism(s) will be addressed below.

2. RT-PCR Studies

Quantitative real-time RT-PCR experiments were conducted using U937 cells that had been made to adhere on PE:N materials for up to 24 h, in order to provide insight into the mechanism(s) of adhesion. We now examine the responses of genes that are known to play important roles in the cell biology of monocytes and macrophages. It is important to note that mRNA expression does not always correlate to protein expression. However, the expression of TNF- α and IL-1 β ,³⁸ as well as PPAR- γ ,³⁹ ICAM-1,^{40,41} and Egr-1,⁴² is primarily regulated at the level of transcription, and their mRNA expression therefore represents a good indicator of their protein expression.

Since cytokines play a central role in the macrophage host defense,⁴³ we investigated the effect of U937 monocyte attachment to PE:N surfaces on the expression of tumor necrosis factor- α (TNF- α) and interleukin-1 beta (IL-1 β), two cytokines secreted as part of immediate early response genes of these cells. The results of these RT-PCR experiments are presented in Fig. 5, and they show a rapid (3 h) but transient stimulatory effect of the amine-rich surfaces on the expression of these genes, attaining 10–15 times and 7–9 times the control values for TNF- α and IL-1 β , respectively. However, the return to control values within 24 h suggests that major inflammatory reactions were thereby not induced, contrary to what was observed for corrosion products of orthopedic implants that induced the expression of TNF- α in U937 cells for at least 24 h under similar

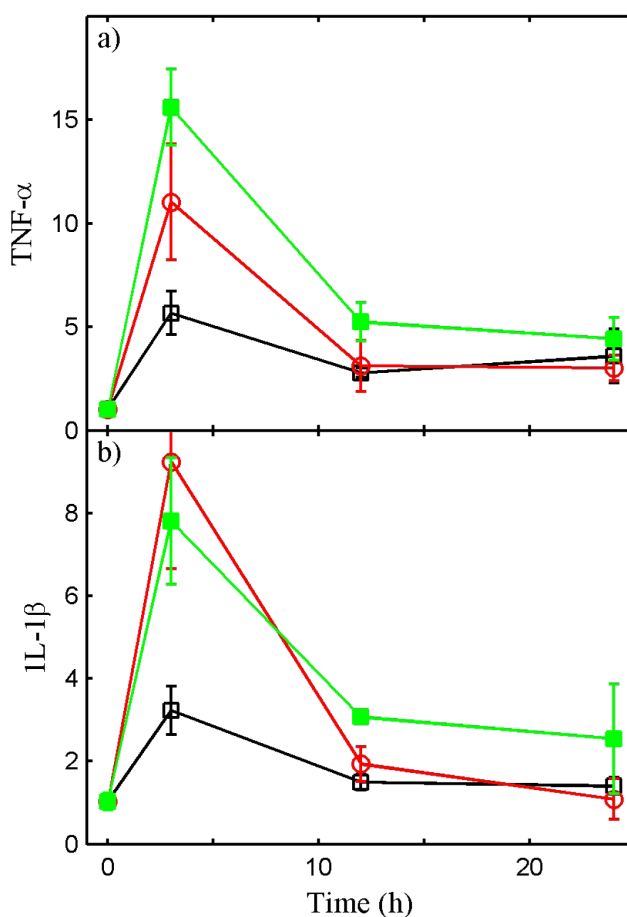


FIGURE 5. Expression of cytokines in U937 monocytes: U937 cells were cultured for up to 24 h in suspension (\square), and adhered on H-PPE:N (\circ) and L-PPE:N (\blacksquare) surfaces with $[\text{NH}_2] \geq [\text{NH}_2]_{\text{crit}}$. Results shown are the mean values \pm standard error of three experiments. * $p < 0.05$ vs. suspension control. (After ref. 13, with permission.)

in vitro conditions.³⁰ However, further long-term adhesion studies are required to prove beyond doubt the low inflammatory reaction of these surfaces toward U937 cells.

C. Human MSCs

A current drawback of cartilage and intervertebral disc (IVD) tissue engineering is that human MSCs from OA patients express COL X,^{14,15,32} a marker of chondrocyte hypertrophy associated with endochondral ossification.^{33,34} Until very recently, no study had addressed the possible effect of the culture substratum on the expression of genes related to hypertrophy. As will be shown presently, results of the study briefly sketched here, but reported in far more detail elsewhere,¹⁵ strongly suggest that MSCs obtained from these patients, a clinically relevant source of stem cells, can be used to engineer cartilage and IVD *in vitro* when precultured on PE:N surfaces and transferred to pellet cultures.

The results of RT-PCR analyses of mRNA expression of type X collagen (COL X) on the different surfaces are shown in Fig. 6. Expression of COL X, a definitive marker for the hypertrophic chondrocyte phenotype,^{14,15,33} was consistently detectable in MSCs cultured on control (PS) culture dishes (Fig. 6, Ctl). The expression of COL X did not change significantly throughout the 7-d culture period on PS control (results not shown). In contrast, its expression was decreased when cultured on L-PPE:N ($61 \pm 19\%$ of control, $p = 0.02$) and on H-PPE:N ($19 \pm 27\%$ of control, $p = 0.001$) coatings. However, L- and H-PPE:N coatings had no significant effect on the expression of type I collagen (COL I; $p = 0.57$ and 0.60 for L- and H-PPE:N, respectively) and aggrecan (AGG; $p = 0.86$ and 0.14 for L- and H-PPE:N, respectively). As previously reported,³² type II collagen was not expressed in MSCs from OA patients cultured on the different surfaces.

In the more detailed version of this study,¹⁵ we showed for the first time that the inhibition of COL X can be maintained in pellet culture after “reprogramming” MSCs on PE:N surfaces. Importantly, reprogramming was found to have little or no effect on COL I, suggesting that these kinds of coatings show promise for tissue engineering of cartilage and disc tissues. However, the observed decrease of AGG expression remains to be addressed, and ongoing investigation is presently looking at the addition of specific growth factors to maintain AGG expression without increasing COL X expression. Finally, the present results strongly suggest that not only the chemical composition but also the surface morphology of plasma-deposited coatings, more specifically of PE:N films (compare Figs. 3B and 3C), affect the behavior of MSCs (unlike the case of U937, where these had no observable effects, as noted in section III.B.1 above); they also suggest that these surfaces offer promising opportunities for tissue engineering of cartilage and disc.

IV. GENERAL DISCUSSION AND CONCLUSIONS

In the present article we have focused our attention upon the culture of two particular cell types of interest in our orthopedics research program, U937 and MSCs, on different PE:N substrates. In numerous earlier articles from these laboratories that are cited in the

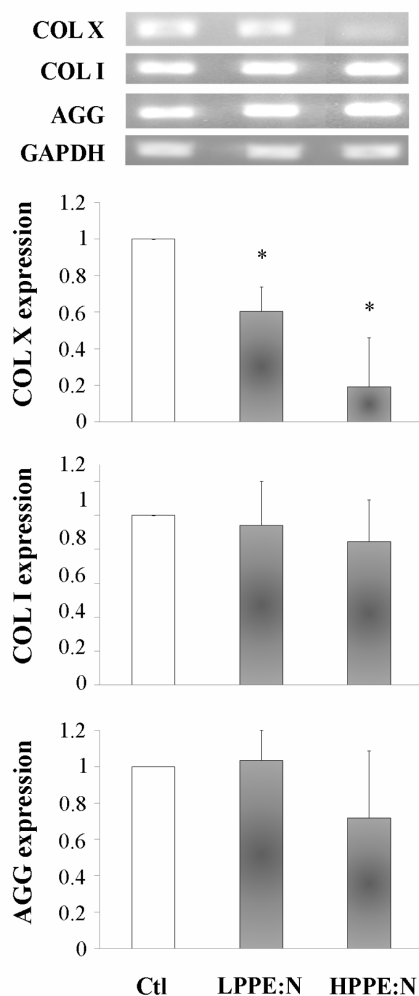


FIGURE 6. Expression of COL X on PS and PPE:N surfaces. MSCs from OA patients were cultured on PS (Control, Ctl), (H50) H-PPE:N, and (L0.75) L-PPE:N for 7 d. Total RNA was extracted and mRNA levels measured by RT-PCR as described in Materials and Methods. GAPDH was used as housekeeping gene and served to normalize the results. Quantitative results are the mean \pm standard deviation of 4 experiments. * $p < 0.05$ vs. PS control. (From ref. 15, with permission.)

list of references, we had already shown that a particular PE:N subgroup, namely H-PPE:N, was also capable of regulating the phenotype of IVD (nucleus pulposus) cells,⁴⁴ of maintaining the phenotypic profile of notochordal cells,⁴⁵ and of promoting healing around stent grafts after endovascular aneurysm repair,⁴⁶ among other applications. In all cases, as in the literature,² those abilities of the coatings were largely attributed to the films' primary amine constituents. We therefore inferred that coatings from another

PE:N subgroup, L-PPE:N, should in principle show even more promise than their H counterparts, on account of their significantly higher amine concentrations, $[\text{NH}_2]$,^{26,28} clearly illustrated in Fig. 2.

First, regarding culture of U937, Fig. 4B clearly shows that the value of $[\text{N}]_{\text{crit}}$ varied widely among the different PE:N materials examined, along with similar coatings based on monomers other than ethylene, from a maximum of 24 at. % to a minimum of 7.5 at. %. The ability to distinguish among the numerous functionalities that contribute to $[\text{N}]$, particularly the primary amine ($-\text{NH}_2$) groups via the use of chemical derivatization, allowed us to identify the key common feature among those various coatings, namely the fact that in all cases $[\text{N}]_{\text{crit}}$ corresponded to a constant value of $[\text{NH}_2]_{\text{crit}}$, 4.2 ± 0.5 (per 100 atoms measured by XPS). Therefore, at least for the case of U937 monocytes, this confirmed the critical role of this ($-\text{NH}_2$) group in cell-surface interactions, something that had earlier been a topic of much uncertainty and debate in the literature.^{1,2} Nevertheless, further studies will be necessary to investigate this critical role of ($-\text{NH}_2$) for the adhesion of other nonadherent cell types.

The data presented in Fig. 5 indicate that the adhesion of U937 monocytes to PE:N surfaces with $[\text{NH}_2] \geq [\text{NH}_2]_{\text{crit}}$ induced a transient expression of $\text{TNF-}\alpha$ and $\text{IL-1}\beta$, two cytokines secreted as part of immediate early response genes of these cells, suggesting that major inflammatory reactions were not induced. In contrast, $\text{PPAR}\gamma$, implicated in the adhesion and retention of monocytes, had a more sustained expression (data shown elsewhere¹³). It was reported in the literature that $\text{PPAR}\gamma$ can be induced in various cell types by $\text{TNF-}\alpha$ and IL-1 ,^{47,48} this would suggest that the transient expression of $\text{TNF-}\alpha$ and IL-1 may induce adhesion of monocytes via the activation of $\text{PPAR}\gamma$, but that was not investigated directly.

Now turning to the second example, MSCs, referring to Fig. 6 and to the preceding discussion regarding U937 cells, it was surprising to note that COL X suppression was *less* prominent in the case of the $[\text{NH}_2]$ -richer (L0.75) L-PPE:N coating than on (H50) H-PPE:N (see Fig. 2). In other words, our anticipated result that the extent of COL X suppression should be directly related to $[\text{NH}_2]$ was not borne out by the observed data. However, as shown in Fig. 3, the L- and H-PPE:N coatings differed not only in their compositions, but also in their surface morphologies. It is well known from the literature that the behavior of cells adhering to solid surfaces can be strongly affected both by the surfaces' chemistries as well as their topological characteristics, particularly by micro-roughness.⁴⁹ Surface roughness-related effects are encountered not only in the case of plasma polymers, but they were, for example, also suggested as a key factor for inducing a favorable osteoblastic behavior of MSCs cultured on different hydroxyapatite deposits on titania (TiO_2) powder.⁵⁰ Now, since the chemical compositions (in terms of $[\text{NH}_2]$) of L0.75 and H50 coatings are not *drastically* dissimilar, and since the latter manifested enhanced capability to reduce COL X expression (Fig. 6), it is conceivable that the morphological differences observed (Fig. 3) play a significant, possibly dominant, role in the control of COL X expression. The apparent synergy between surface composition and morphology on MSC regulation remains to be elucidated, and this is now the object of further in-depth investigation.

ACKNOWLEDGMENTS

The authors gratefully acknowledge financial support from the Canadian Institutes of Health Research (CIHR), the AO Foundation (Switzerland), NanoQuebec, and the Natural Sciences and Engineering Research Council of Canada (NSERC).

REFERENCES

1. Förch R, Zhang Z, Knoll W. Soft plasma treated surfaces: tailoring of structure and properties for biomaterial applications. *Plasma Process Polym.* 2005;2:351–372.
2. Siow KS, Britcher L, Kumar S, Griesser HJ. Plasma methods for the generation of chemically reactive surfaces for biomolecule immobilization and cell colonization—a review. *Plasma Process Polym.* 2006;3:392–418.
3. Special Issue: Plasma Medicine. *Plasma Process Polym.* 2010;7(3,4).
4. Wertheimer MR, Martinu L, Klemberg-Sapieha JE, Czeremuszkin G. Plasma Treatment of Polymers to Improve Adhesion. In K.L. Mittal and A. Pizzi, editors, *Adhesion Promotion Techniques in Advanced Technologies*. New York: Marcel Dekker; 1998, pp. 139–174.
5. Truica-Marasescu F, Wertheimer MR. Vacuum ultraviolet–induced photochemical nitriding of polyolefin surfaces. *J Appl Polym Sci.* 2004;91:3886–3898.
6. Griesser HJ, Chatelier RC, Gengenbach TR, Johnson G, Steele JG. Growth of human cells on plasma polymers: putative role of amine and amide groups. *J Biomater Sci, Polym Ed.* 1994;5:531–554.
7. Girard-Lauriault P-L, Mwale F, Iordanova M, Demers C, Desjardins P, Wertheimer MR. Atmospheric pressure deposition of micropatterned N-rich plasma-polymer films for tissue engineering. *Plasma Process Polym.* 2005;2:263–270.
8. Girard-Lauriault P-L, Desjardins P, Unger WES, Lippitz A, Wertheimer MR. Chemical characterisation of nitrogen-rich plasma-polymer films deposited in dielectric barrier discharges at atmospheric pressure. *Plasma Process Polym.* 2008;5:631–644.
9. Friedrich J, Kühn G, Mix R, Fritz A, Schönhals A. Polymer surface modification with mono-functional groups of variable types and densities. *J Adhes Sci Technol* 2003;17:1591–1617.
10. Oran U, Swaraj S, Lippitz A, Unger WES. In-situ characterization of plasma-deposited allylamine films by ToF-SIMS, XPS and NEXAFS spectroscopy. *Plasma Process Polym.* 2006;3:288–298.
11. Shard AG, Whittle JD, Beck AJ, Brookes PN, Bullett NA, Talib RA, Mistry A, Barton D, McArthur SL. A NEXAFS examination of unsaturation in plasma polymers of allylamine and propylamine. *J Phys Chem B.* 2004;108:12472–12480.
12. Bullett NA, Bullett DP, Truica-Marasescu F-E, Lerouge S, Mwale F, Wertheimer MR. Polymer surface micropatterning by plasma and VUV-photochemical modification for controlled cell culture. *J Appl Surf Sci.* 2004;235:395–405.
13. Girard-Lauriault P-L, Truica-Marasescu F, Petit A, Wang HT, Desjardins P, Antoniou J, Mwale F, Wertheimer MR. Adhesion of human U937 monocytes to nitrogen-rich organic thin films: novel insights into the mechanism of cellular adhesion. *Macromol Biosci.* 2009;9:911–921

14. Mwale F, Girard-Lauriault P-L, Wang HT, Lerouge S, Antoniou H, Wertheimer MR. Suppression of genes related to hypertrophy and osteogenesis in committed human mesenchymal stem cells cultured on novel nitrogen-rich plasma polymer coatings. *Tissue Eng.* 2006;12:2639–2647.
15. Rampersad S, Ruiz J-C, Petit A, Antoniou J, Wertheimer MR, Mwale F. Stem cells, nitrogen-rich plasma-polymerized culture surfaces and type x collagen suppression. *Tissue Eng Part A*: 2011;17: 2551-2560.
16. Nebe B, Finke B, Lüthen F, Bergemann C, Schröder K, Rychly J, Liefelth K, Ohl A. Improved initial osteoblast functions on amino-functionalized titanium surfaces. *Biomol Eng.* 2007;24:447–454.
17. Zhang Z, Chen Q, Knoll W, Förch R. Effect of aqueous solution on functional plasma polymerized films. *Surf Coatings Technol.* 2003;174–175:588–590.
18. Vasilev K, Britcher L, Casanal A, Griesser HJ. Solvent-induced porosity in ultrathin amine plasma polymer coatings. *J Phys Chem B.* 2008;112:10915
19. Tarasova A, Hamilton-Brown P, Gengenbach T, Griesser HJ, Meagher L. Colloid probe AFM and XPS study of time-dependent aging of amine plasma polymer coatings in aqueous media. *Plasma Process Polym.* 2008;5:175–185.
20. Denis L, Cossement D, Godfroid T, Renaux F, Bittencourt C, Snyders R, Hecq M. Synthesis of allylamine plasma polymer films: correlation between plasma diagnostic and film characteristics. *Plasma Process Polym.* 2009;6:199–208.
21. Finke B, Schröder K, Ohl A. Structure retention and water stability of microwave plasma polymerized films from allylamine and acrylic acid. *Plasma Process Polym.* 2009;6:S70–S74.
22. Hegemann D, Hossain M-M. Influence of non-polymerizable gases added during plasma polymerization. *Plasma Process Polym.* 2005;2:554–562.
23. Hossain M-M, Herrmann AS, Hegemann D. Incorporation of accessible functionalities in nanoscaled coatings on textiles characterized by coloration. *Plasma Process Polym.* 2007;4:135–144.
24. Hegemann D, Hossain M-M, Körner E, Balazs DJ. Macroscopic description of plasma polymerization. *Plasma Process Polym.* 2007;4:229–338.
25. Truica-Marasescu F-E, Wertheimer MR. Nitrogen-rich plasma-polymer films for biomedical applications. *Plasma Process Polym.* 2008;5:44–57.
26. Truica-Marasescu F, Wertheimer MR. Vacuum-ultraviolet photopolymerisation of amine-rich thin films. *Macromol Chem Phys.* 2008 ;209 :1043–1049. Erratum: 2008;209 :2061.
27. Sarra-Bournet C, Gherardi N, Glénat H, Laroche G, Massines F. Effect of C₂H₄/N₂ ratio in an atmospheric pressure dielectric barrier discharge on the plasma deposition of hydrogenated amorphous carbon-nitride films (a-C:N:H). *Plasma Chem Plasma Process.* 2010;30:213–239.
28. Ruiz JC, St-Georges-Robillard A, Thérésy C, Lerouge S, Wertheimer MR. Fabrication and characterisation of amine-rich organic thin films: focus on stability. *Plasma Process Polym.* 2010;7:737–753.
29. Truica-Marasescu F, Girard-Lauriault P-L, Lippitz A, Unger WES, Wertheimer MR. Nitrogen-rich plasma polymers: comparison of films deposited in atmospheric- and low-pressure plasmas. *Thin Solid Films* 2008;516:7406–7417.

30. Luo L, Petit A, Antoniou J, Zukor DJ, Huk OL, Liu RCW, Winnik FM, Mwale F. Effect of cobalt and chromium ions on MMP-1, TIMP-1, and TNF-alpha gene expression in human U937 macrophages: a role for tyrosine kinases. *Biomaterials* 2005;26:5587–5593.
31. Gong YK, Luo L, Petit A, Huk O, Antoniou J, Winnik FM, Mwale F. Adhesion of human U937 macrophages to phosphorylcholine-coated surfaces. *J Biomed Mater Res.* 2005;72A:1–9.
32. Nelea V, Luo L, Demers CN, Antoniou J, Petit A, Lerouge S, Wertheimer MR, Mwale F. Selective inhibition of type X collagen expression in human mesenchymal stem cell differentiation on polymer substrates surface-modified by glow discharge plasma. *J Biomed Mater Res* 2005;75A:216–223.
33. Mwale F, Billinghamurst C, Wu W, Alini M, Webber C, Reiner A, Ionescu M, Poole J, Poole AR. Selective assembly and remodelling of collagens II and IX associated with expression of the chondrocyte hypertrophic phenotype. *Dev Dyn* 2000;218:648–662.
34. Poole AR, Lavery S, Mwale F. Endochondral bone formation and development in the axial and appendicular skeleton. In Henderson JE, Galtzman D, editors. *The Osteoporosis Primer*, Cambridge, UK: Cambridge University Press; 2000. pp. 3–17.
35. Ruiz JC, Girard-Lauriault PL, Truica-Marasescu F, Wertheimer MR. Plasma- and vacuum-ultraviolet (VUV) photo-polymerisation of N- and O-rich thin films. *Rad Phys Chem.* 2010;79:310–314.
36. Jaiswal N, Haynesworth SE, Caplan AI, Bruder SP. Osteogenic differentiation of purified, culture-expanded human mesenchymal stem cells *in vitro*. *J Cell Biochem.* 1997;64:295–312.
37. Chomczynski P, Sacchi N. Single-step method of RNA isolation by acid guanidinium thiocyanate-phenol-chloroform extraction. *Anal Biochem.* 1987;162:156–159.
38. Mitschik S, Schierl R, Nowak D, Jörres RA. Effects of particulate matter on cytokine production *in vitro*: a comparative analysis of published studies. *Inhal Toxicol.* 2008;20:399–414.
39. Ahn KO, Lim SW, Yang HJ, Li C, Sugawara A, Ito S, Choi BS, Kim YS, Kim J, Yang CW. Induction of PPAR gamma mRNA and protein expression by rosiglitazone in chronic cyclosporine nephropathy in the rat. *Yonsei Med J.* 2007;48:308–316.
40. Yang P-Y, Rui Y-C, Huang X-H, Jiang J-M. Expression of intercellular adhesion molecule-1 in U937 foam cells and the inhibitory effect of imperatorin. *Acta Pharmacol Sin.* 2002;23:327–330.
41. Benson V, McMahon AC, Lowe HC. ICAM-1 in acute myocardial infarction: a potential therapeutic target. *Current Mol Med.* 2007;7:219–227.
42. Shao H, Kono DH, Chen L-Y, Rubin EM, Kaye J. Induction of the early growth response (Egr) family of transcription factors during thymic selection. *J Exp Med.* 1997;185:731–744.
43. Bendtzen K. Interleukin 1, interleukin 6 and tumor necrosis factor in infection, inflammation and immunity. *Immunol Lett.* 1988;19:183–192.
44. Mwale F, Petit A, Tian Wang H, Epure LM, Girard-Lauriault PL, Ouellet JA, Wertheimer MR, Antoniou J. The potential of N-rich plasma-polymerized ethylene (PPE:N) films for regulating the phenotype of the nucleus pulposus. *Open Orthop J.* 2008;2:137–144.
45. Mwale F, Wang HT, Petit A, Girard-Lauriault PL, Hunter CJ, Ouellet JA, Wertheimer MR, Antoniou J. The effect of novel nitrogen-rich plasma polymer coatings on the phenotypic profile of notochordal cells. *Biomed Eng Online.* 2007;6:33.

46. Lerouge S, Major A, Girault-Lauriault P-L, Raymond M-A, Laplante P, Soulez G, Mwale F, Wertheimer MR, Hébert M-J. Nitrogen-rich coatings for promoting healing around stent-grafts after endovascular aneurysm repair. *Biomaterials*. 2007;28:1209–1217.
47. Pigott R, Dillon LP, Hemingway IH, Gearing AJ. Soluble forms of E-selectin, ICAM-1 and VCAM-1 are present in the supernatants of cytokine activated cultured endothelial cells. *Biochem Biophys Res Commun*. 1992;197:584–589.
48. Pober JS, Lapierre LA, Stolpen AH, Brock TA, Springer TA, Fiers W, Bevilacqua MP, Mendrick DL, Gimbrone MA Jr. Activation of cultured human endothelial cells by recombinant lymphotoxin: comparison with tumor necrosis factor and interleukin 1 species. *J Immunol*. 1987;138:3319–3324.
49. Di Mundo R, Gristina R, Sardella E, Intranuovo F, Nardulli M, Milella A, Palumbo F, d'Agostino R, Favia P. Micro-/nanoscale structuring of cell-culture substrates with fluoro-carbon plasmas. *Plasma Process Polym*. 2010;7:212–223.
50. Lima RS, Dimitrievska S, Bureau MN, Marple A, Petit A, Mwale F, Antoniou J. HVOF-sprayed nano TiO₂-HA coatings exhibiting enhanced biocompatibility. *J Thermal Spray Tech*. 2010;19:336–343.

